Volume Number 10 || Issue Number 1 || Year 2025 || Page 25 || * Corresponding Author: arshad.iqbal@uswat.edu.pk||

ISSN (Online) = 2522-6754 ISSN (Print) = 2522-6746

WORLD JOURNAL OF BIOLOGY AND BIOTECHNOLOGY

Research Manuscript www.sciplatform.com Peer review

A computational immune-informatics approach to design multi-epitope vaccine against *Guanarito virus* targeting nucleoprotein and nucleo-capsid proteins

Itazaz Ul Haq, Najeebullah, Muhammad Rahiyab, Syed Shujait Ali, Ishaq Khan, Zahid Hussain, Arshad Iqbal *

Centre for Biotechnology and Microbiology, University of Swat, Mingora 19200, KPK, Pakistan

Contribution | **Haq, I**, & **Najeebullah** conducted data collection and analysis using software, wrote methodology, **M. Rahiyab**, **S. S. Ali**, **I. Khan**, & **Z. Hussain** performed computational simulations and validated results, and **A. Iqbal** supervised the research and manuscript preparation.

ABSTRACT

The human *Guanarito virus* (*GTOV*), belongs to the order Bunyavirales and family Arenaviradae, was found in the Portuguese state of Portugal's Guanarito municipality. Due to its seasonal occurrence, Venezuelan haemorrhagic fever was caused by severe haemorrhagic febrile sickness outbreak happened in 1989. The lack of antiviral medications or vaccines to prevent the *GTOV* infection means that the treatment for *GTOV* infection is currently uncertain; thus, the development of an efficacious vaccine is imperative. Within this research, immune-informatics approaches were utilized to develop an effective vaccine candidate to combat with *GTOV* infections. We retrieve the nucleo and nucleo-capsid proteins of the *GTOV* from the National Center for Biotechnology Information database and forecast HTL, B-cell, and CTL epitopes against these proteins using different tools. Non-allergenic and antigenic epitopes were coupled with suitable linker, like KK, GPGPG, and AAY. Furthermore, an adjuvant HMAN Beta-defensin was added to the C-terminal end of the vaccine via EAAAK linker. Using the SoluProt tool, the vaccine solubility value of 0.7951 was produced. Additionally, the vaccine was projected to have an antigenicity score of 0.929968, an immunogenicity score of -0.22436, and a non-toxic and nom-allergenic reaction. It was determined that the vaccine's ERRAT value was 97.368%, 89.0% of residues were in the most favoured region, 9.6 % were in the additional allowed zone, and 0.4% were in the generously allowed region, according to the Ramachandran plot. While the vaccine's Z-score was calculated to be -4.8. Experimental validation is required to establish the efficacy of this vaccine, with further testing needed to demonstrate its safety and immunogenicity for treating *GTOV* related disorders. Overall, this study highlights the potential of computational vaccine design as a promising approach to combat *GTOV* infections, paving the way for future experimental validation and development of an effective therapeutic strategy.

Keywords: *Guanarito virus*, epitopes prediction, multi-epitopes vaccine construct, MD simulation, immune simulation.

INTRODUCTION: The *Guanarito virus*, also known as the Mammarenavirus, belongs to the order Bunyavirales and family Arenaviradae, it's an RNA virus with a negative strand (Silva-Ramos *et al.*, 2022). Both old world and new world arenaviruses are members of this genus. The tacaribe complex of viruses, which comprises the Arenaviruses of the New world, to which *GTOV* is related, is divided: Clade : A, B, C, and A/Rec (Charrel *et al.*, 2008). Clade B comprises human-pathogenic new world arenaviruses, such as the *Chapare virus* (*CHAPV*), *Machupo* (*MACV*), *MACV* is the agent responsible for Bolivian haemorrhagic fever, while the *CHAPV* cause Chapare haemorrhagic fever, the underlying cause of Brazilian haemorrhagic fever is the *Sabia virus* (*SABV*), and the *GTOV*, which causes Venezuelan haemorrhagic fever (VHF) (Radoshitzky *et al.*, 2018). Portuguesa state in Venezuela and its surrounding areas were the first to report an epidemic of VHF, with a fatality rate, 60% confirmed cases of 60% (9/15) (Manzione *et al.*, 1998). After September 1989, saw a fatal case yielded the first strain of *GTOV*, subsequent investigation demonstrated that this virus was distinct within the tacribe complex (Cline *et al.*, 2023). Another arenavirus known as *Pirital virus* (*PIRV*), which was identified in 1997, is extensively transmitted in rural regions where *GTOV* is also prevalent (Milazzo *et al.*, 2011), However, *PIRV*-related human instances are still unknown. The limited distribution of Zygodontomys brevicauda, the rodent reservoir host, in western Venezuela may be the cause of the geographical fecality of VHF (Mills and Childs, 2001). Though its exact cause is unknown, it has been suggested that human migration and changed land use practices in areas of abandoned forest in the states of Portugal and Barinas contributed to the development of VHF. Grassland mice, including Z. brevicauda, flourished as fields and pastures took the place of forested areas, increasing the likelihood of interaction between vulnerable people and sick rats with *GTOV* (Dufour, 2021). However, because of recent alterations in the social and environmental spheres, such as migration, deforestation, and population growth (Swain, 1996), The number of instances may have been overestimated and *GTOV* may be a significant contributor to acute undifferentiated febrile sickness in the surrounding areas. The about 9000 Km that compose the VHF endemic region inside Venezuela are the south and southwest regions of the state of Portuguesa and neighbouring areas, mostly in the state of Barinas (Lendino *et al.*, 2024). Tropical weather prevails in these areas, with a mean yearly temperature of 28°C, 1300 mm of precipitation on average, with heavier seasonal rainfall from May to November and a dry season from December to April (Camberlin, 2018). Only the states of Portugal and Barinas have reported human VHF cases linked to the *Guanarito virus* (Wahl-Jensen *et al.*, 2013). The municipality of Guanarito in Portuguesa state, Venezuela experienced an outbreak of severe haemorrhagic febrile sickness in September 1989. It is believed that this outbreak initial case of infection with *GTOV* documented in the scientific literatures (Qi *et al.*, 2024). No reports regarding prior cases could be located, even though prior to the 1989 epidemic, local physician had documented comparable clinical cases (Bell *et al.*, 1981). The Venezuelan Health Ministry was notified of 104 probable cases and 26 fatalities that were found during surveillance in the same municipality between 1990 and 1991 (Guajira, 1995). Fifteen of these patients had a confirmed diagnosis of VHF following their admission and care at the Miguel Oraa hospital in Guanare (Silva-Ramos *et al.*, 2022). Serum samples were taken in 1991 from family contacts of patients with confirmed VHF cases in order to ascertain the patients' exposure to *GTOV*. According to the study, 10.5% of participants exhibited antibodies against *GTOV*, which may indicate a moderate case of VHF (Racsa *et al.*, 2016). Due to potential VHF cases that were happening in this and other surrounding towns, after a year in 1992, a second serological investigation was carried out in the state of Portuguesa in the community of La Hoyada. However the study found that among residents, there was low seroprevalence of *GTOV* antibodies 3.6% (Silva-Ramos *et al.*, 2022). A total of 165 suspected cases have been recorded since *GTOV* was identified as the etiological agent of VHF 1989 to 1997, of which only 40% have been verified by viral isolation and/or seroconversion detection (Silva-Ramos *et al.*, 2022). Despite the fact that VHF instances were reported monthly, November, December, and January accounted for more than half of these cases (Organization, 2016). From September 1989 through August 1992, cases were continuously recorded; after that, the numbers decreased until August 1996, when there was no evidence of disease activity; nevertheless, from August 1996 to May 1997, the number of VHF cases climbed once more(Hayward, 2015). According to the latest recent data, 618 VHF cases with a case-fatality rate of 23.1% were reported in the state of Portugal between September 1989 and December 2006 (Blumberg *et al.*, 2014). The lack of epidemiological research and an inadequate surveillance system in Venezuela have led to little information about the total number of illnesses from 2006 and 2021, when a recent study found 36 confirmed cases (Barreto *et al.*, 2024). Owing to the infection's quick onset and high fatality rates, *GTOV* is considered a high-priority category by the CDC. A biological warfare agent (Elumalai and McKee, 2021). Biosafety level 4 laboratories are the only places where it is permitted to be modified (Organization, 2004). All confirmed and suspected cases of VHF involved individuals who

were either residents of the endemic zone or those who did not live there but had recently visited (Shoemaker, 2019); As a result, being in an endemic area may increase the risk of contracting *GTOV*. The group most at risk is males of reproductive age because of occupational exposure to rodents carrying the infection, such as the cane mice with short tail, Z.brevicauda, which prevent untamed and remote regions (Loyd, 2015). Drawing from 165 VHF cases data from September 1989 to January 1997, the bulk of cases occurred during November and January, coinciding with the peak agricultural activity in the region and the end of the season of rain (Gerken *et al.*, 2021). Surprisingly, in 1998, the principal source of income for almost half of the residents in those rural areas was agriculture and/or livestock husbandry. But throughout the seasons of planting and harvesting, a large number of momentary farming migrants from Venezuela and the adjacent Colombia visit VHF endemic areas in search of work (Enria, 2005), putting one at risk for *GTOV* infection. Although wild rats are highly transmissible, there has only been one likely secondary case published in the scientific literature, implying that there may not be many occurrences of VHF caused by inter human transmission (Silva-Ramos *et al.*, 2022). Following a 3-12 days incubation period, arthralgia, fever, headache, sore throat, cough, nausea, vomiting, diarrhea, bleeding gums, menorrhagia, and melena are the most common early symptoms (Kahan, 2008). Most individuals have leukopenia and thrombocytopenia when they first arrive. Assessment of other laboratory markers is useless, and there is no correlation between the platelet count and the clinical outcome (Zarychanski and Houston, 2017). When severe symptoms first appear, patients are typically very sick and frequently dehydrated and sleepy. Diffuse pulmonary edema and haemorrhagic congestion are typically the causes of death, while those who survive typically recover without any aftereffects. On the other hand, convalescence is drawn out and necessitates extended hospital stays. Cases of VHF and other Arena viral haemorrhagic fevers are similar clinically. Most patients with VHF report a fever and a progressive onset of symptoms, and the illness frequently starts off as a low-grade fever without specific symptoms that worsens over the course of six days. The most common haemorrhagic signs in patient with severe sickness include melena, hematemesis, petechiae, epistaxis, and rectal bleeding (Moraz and Kunz, 2011). Overall, depending on early intervention and treatment, the case fatality rate might be as high as 33.3%; however, the prognosis is poorer in patients with a current or recent history of convulsions (Ghani *et al.*, 2005).

The lack of effective antiviral drugs or a vaccine to confer immunity makes treatment for *GTOV* is unclear (Silva-Ramos *et al.*, 2022). For this reason, this study used computational analysis to predict epitopes for a potential *GTOV* vaccine. Using pre-established criteria for choosing possible epitopes for the final vaccine design, T Cell, B Cell, and HTL epitopes were predicted and assessed. The ultimate vaccine construct's potential was validated by additional use of codon optimization for expression, TLR receptor based molecular docking and molecular dynamic simulation. As a result, this work presents a strategy for creating a viable vaccine candidate to prevent *GTOV*.

OBJECTIVES: The objectives of this study involve employing algorithms to identify and assess relevant proteins from the *GTOV*, aiding in the formulation of a better vaccine. Advanced immune-informatics techniques are used to predict the epitope characteristics of HTL, CTL, and B-cells, which are crucial for vaccine design. Computational modelling and verification are then applied to ensure the stability and compatibility of the vaccine candidate. Additionally, *in-silico* immune simulations and molecular dynamics analysis are conducted to assess the vaccine's immunogenicity while considering its structural stability. Finally, the vaccine construct is duplicated *in-silico* into an appropriate expression vector, preparing it for experimental testing.

MATERIALS AND METHODS: Figure 1 illustrate the complete procedure of this work.

Protein collection of *GTOV*: From the database of NCBI (https://www.ncbi.nlm.nih.gov), two *GTOV* proteins, nucleoprotein and nucleo-capsid, were extracted (Fernandes *et al.*, 2018). The server of VaxiJen (http://www.ddg-pharmfac.net/vaxigen/vaxigen/vaxigen.html) recognized these proteins as antigenic, and they were chosen for the creation of vaccine (Doytchinova and Flower, 2007).

The T-cell (CTL) epitopes prediction: This web-based program (NetCTL 1.2 - DTU Health Tech - Bioinformatic Services) predicts CTL epitopes against these proteins (Bhattacharjee *et al.*, 2023). The accuracy of transporter associated with antigen processing (TAP) transport, proteasomal C-terminal degradation efficiency, and peptide binding to MHC are three critical elements that influence the prediction of these CTL epitopes. Peptide binding to MHC 1 and proteasomal C-terminal degradation prediction was done using an artificial neural network, whilst a weight matrix was used to predict the TAP transport score. The threshold for CTL epitopes identification were set at 0.75 (Larsen *et al.*, 2007).

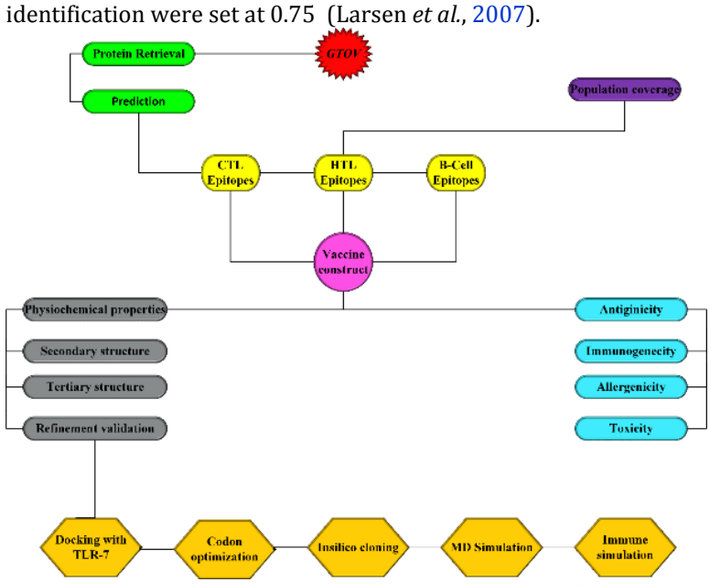

Figure 1: Stages in the creation of an epitope-based vaccine to combat with *GTOV* infections are shown diagrammatically.

Helper T-cell epitopes prediction: With a 15-mer length for seven human alleles, the helper T lymphocytes (HTL) With the use of the online IEBD server (https://www.iedb.org/) (Fadaka *et al.*, 2021), the seven HLA allele reference set HLA-*03:01, HLA-*07:01, HLA-*15:01, HLA-*01:01, HLA-*02:02, HLA-*04*01:01, and HLA-*5*01:01 were predicted for the *GTOV* nucleo and nucleo-capsid proteins. The IC50 value given to each epitope determines the affinity of peptides for the relevant receptors. An IC50 value of less than 50 nM is required for peptides with higher binding affinities, while IC50 values of less than 500 nM and less than 5000 nM denote intermediate and low binding affinities, respectively. The percentile rank score and the epitope's binding affinity are negatively correlated; that is, higher binding affinities are correlated with lower percentile rankings.

The B-Cell epitopes prediction: Because they can induce humoral immunity by being detected via B-Cells receptors or antibodies generated, B-cell epitopes play a critical role in initiating an effective defence mechanism. Consequently, it is important for the host antibody production strategy that these epitopes be present in the vaccine design (Abbott and Crotty, 2020), ABCpred (https://webs.iiitd.edu.in/raghava/abcpred/ABC_submission.html) is an online server that we used to predict linear or continuous B cell epitopes. ABCpred can predict linear B-cell epitopes with a sensitivity of 0.49 and a specificity of 0.75, and it has a precision rate of 75% (Mahapatra *et al.*, 2023).

Analysis of population coverage: We carried out a comprehensive investigation of the population coverage of particular epitopes using the population coverage analysis program on the IEDB server (https://www.iedb.org/) (Liang *et al.*, 2021). We uploaded the combined MHC-II epitope data to ensure the most thorough study possible, and our selection procedure was created to take into account all parts of the world. We employed the default parameters and verified the accuracy of our results by cross-referencing the coverage with the HLA class II binding alleles.

Multi-epitope vaccine construction: B-cell, CTL, and HTL epitopes were successfully separated from the high-score epitopes using a variety of criteria. With extreme precision, the final multi-epitope subunit vaccine was subsequently constructed using the chosen epitopes. AAY, GPGPG, and KK were among the several linkers that was used to join the chosen epitopes (Umar *et al.*, 2021). Linkers have two important functions: they help bind HLA-II epitopes and aid in immunological processing. They also indicate the cleavage site, which reduces the total number of epitopes (MacLachlan *et al.*, 2019; Rahmani *et al.*, 2019). The adjuvant HUMAN Beta-defensin 103 (UniProt ID: P81534) was introduced at the C-terminal end of

the vaccine sequence in order to improve the vaccine's consistency and immunogenic response (Hervé *et al.*, 2019).

Vaccine allergenicity prediction: Utilizing the Allertop 2.0 (https://www.ddg-pharmfac.net/AllerTOP/) web tool, the non-allergenic potential of a multi-epitope subunit vaccine was predicted (Abraham Peele *et al.*, 2021).

Antigenicity profiling of vaccine: In order to ascertain the antigenic character of a vaccine protein, the complete vaccine was sent for analysis to the VaxiJen v2.0 server (http://www.ddg-pharmfac.net/vaxijen/) (Almofti *et al.*, 2021). Also Antigenicity forecasting was done using the web server ANTIGENpro (http://scratch.proteomics.ics.uci.edu/) (Rahman *et al.*, 2019). The protein antigenicity prediction server used a two-pronged strategy: Protein antigenicity machine-learning algorithms were deployed in addition to repeatedly repeating the core protein sequence in order to produce a conclusion based on analysis of protein microarray data.

Physical and chemical characteristics identification of final vaccine protein: The Grand Average of Hydropathicity (GRAVY) as well as the theoretical isoelectric point, stability index, composition of amino acids, half-lives *in vivo* and *in vitro* molecular mass, and aliphatic index were all forecasted using ProtParam (http://web.expasy.org/protparam/), an online platform (Bhagwat *et al.*, 2021).

Multi-epitope vaccine solubility rate: Software called SOLUPROT available online was utilizes to assess the multi-epitope vaccine in its final form design (https://loschmidt.chemi.muni.cz/soluprot/). A solubility score was produced by the tool, which employs various scores. Protein solubility in *Escherichia coli* is suggested by a score below 0.5, which is denoted by a red hue. A score above 0.5 indicates that the protein is likely to be soluble (Ahmad *et al.*, 2024).

Prediction of the final subunit vaccine's secondary structure: To calculate the vaccine construct's secondary structure, the PSIPRED web server (http://bioinf.cs.ucl.ac.uk/psipred/) was used (Obaidullah *et al.*, 2021). This technique, which is well-known for its great accuracy, examines using two feed-forward neural networks position-specific integrated-BLAST (PSI-BLAST) data (Ismail, 2015). Alpha helices, protein folds, transmembrane topology, membrane helix prediction, domain recognition, and secondary structure are among the structural properties that the web server PRISPRED can reliably predict (Kader *et al.*, 2022).

Tertiary structure prediction of the final vaccine design: The creation of a three-dimensional vaccine model is one of the most important phase in the development of an epitope-based vaccine. The vaccine's protein sequence was sent to the Robetta Server in FASTA format so that it could be subjected to three-dimensional structural analysis. To ensure correctness, use Continuous Automated Model Evaluation (CAMEO), the server Robetta (https://robetta.bakerlab.org/) has been recognized as the most accurate server since 2014 (Singh *et al.*, 2023).

Refinement of the structure: The amino acids sequence dictates this three-dimensional structure is essential to the function of the protein. These elements control how proteins interact with additional body components such as enzymes, receptors, and antibodies (Alberts *et al.*, 2002). As such, the three dimensional structure of a vaccine protein may influence its capacity to elicit an immunological response and provide protective immunity (Bachmann and Jennings, 2010). An online tool called Galaxy Refine (https://galaxy.seoklab.org/cgi-bin/submit.cgi?type=REFINE) was used to optimize the three-dimensional structure of the suggested multi-epitope subunit vaccine (Hozori *et al.*, 2023). As well as the percentage of favoured areas in the ramachandran plot and the GDT-HA, MolProbity, Clash, RMSD, and Poor rotamers, the Galaxy Refine output shows scores for each of the five created structure models. Utilizing the CASP10 refinement technique, this tool reconstructs and repackages the side chains of the protein. With the use of Galaxy Refine, one of the most trustworthy server for enhancing the general and local quality of protein structures based on the CASP10 method, the structure created by utilizing the greatest protein structure prediction online tools was further applied (Peng *et al.*, 2023). Galaxy Refine uses molecular dynamics simulations to relax the 3D structure.

Validation of the structure: To confirm the improved vaccine model's structural validity, the web resources ERRAT, PROCHECK, and ProSA-web were utilized. Using the ERRAT web tool, non-covalent interactions between several atoms were examined (Irsal *et al.*, 2024). Using the PROCHECK service, the desired model's validation using Ramachandran plot was carried out, which assessed stereo chemistry characteristics residue by residue (Ravikumar *et al.*, 2019). Energy-favourable area extent is indicated by the scores obtained from the Ramachandran chart. The threshold for an acceptable score is above 85% (Medina, 2022). PROCHECK and ERRAT can be accessed through SAVES version 6 (https://saves.mbi.ucla.edu/). Ultimately, the energy plot and Z-score value, which indicate the target vaccine model's overall quality score, were computed via use of the ProSA-web server (https://prosa.services.came.sbg.ac.at/prosa.php) (Shafaghi *et al.*, 2023). The data are compared to native protein structures ascertained by X-ray crystallography and NMR, and are shown graphically with residues on the x- and Z-scores on the y-axes (Mao *et al.*, 2014).

Discontinuous B-cell epitopes prediction: Discontinuous B-cell epitopes are formed by distant residues in the protein sequence that are brought closer together by protein folding (Ferdous *et al.*, 2019). The ElliPro antibody epitope prediction server (http://tools.iedb.org/ellipro/) uses the protein's 3D structure to identify possible discontinuous or conformational B-cell epitopes (Singh *et al.*, 2021). ElliPro uses three methods based on protrusion index (PI) values to measure the PI of the residues and nearby cluster residues, as well as to estimate the ellipsoidal shape of the protein (Ponomarenko *et al.*, 2008). The default settings for epitope prediction were kept when the selected model in PDB format was submitted to the ElliPro server.

Docking of the vaccine structure with TLR7 and use PDBsum to analyse the complexes: A sustained immunological response can only be elicited by the vaccine material binding with particular immune cell receptors. We studied these connections by using molecular docking studies. By studying the ligand-receptor interaction, molecular docking is a useful method for figuring out the stability and affinity for complex binding (Guedes *et al.*, 2014). To obtain the PDB structure of TLR7 (PDB Code: 7CYN), PDB database of RCSB (https://www.rcsb.org/) was utilized (Matamoros-Recio, 2023). The HDOCK server (http://hdock.phys.hust.edu.cn/) was utilized to upload the examination data in order to look into how the vaccine material and TLR interacted (Kumar *et al.*, 2023). After that, PyMOL was used to visualize the 3D complexes between the vaccine material and TLR. PDBsum was eventually used to map the interaction residues between the vaccine ingredient and the TLR (Khan *et al.*, 2022).

Evaluating the vaccine's binding strength using TLR: The PDBsum web server was utilized to examine the vaccine's binding affinity with TLR7 after docking analysis had determined the best structure for each docked complex. One graphical database that provides an overview of the contents of every 3D structure included in the Protein Data Bank (PDB) is PDBsum (https://www.ebi.ac.uk/thornton-srv/databases/pdbsum/) (Feisal, 2015). Together with illustrations showing their interactions, it shows the molecule or molecules making up the structure, such as DNA, ligands, protein chains, and metal ions (Shamsi and Kraatz, 2013). For a three-dimensional perspective of the molecules and their interactions, the database makes considerable use of the molecular graphics tools PyMOL, JSmol, and RasMol.

The final vaccine design's reverse translation, codon optimization, and *in-silico* cloning: A process known as "Codon adaptation" is used when both organisms use different codons to increase the rate at which the foreign genes are expressed in the host. As a result, the vaccine protein was expressed in *E. coli K12* (Chung and Lee, 2012), the most sequenced prokaryotic organism, using JCAT or the Java Codon Adaptation tool (https://www.jcat.de/) (Kizhakedathil *et al.*, 2022). Using the backtranseq program of EMBOSS reverse (https://www.ebi.ac.uk/Tools/st/embossbacktranseq) to transform the sequence of amino acids to a nucleotide sequence to express a chimeric protein in the expression system (Zaib *et al.*, 2022). The optimal ranges are 0.8–1.0 for the expression rate factors, 30–70% for the codon adaptation index (CAI), and 0.8–1.0 for the percentage of the GC-content codon. One considers a CAI of 1.0 to be the ideal outcome (Ranaghan *et al.*, 2021). The additional JCAT possibilities were examined for the avoidance of bacterial Ribosome binding sites, restriction enzymes cleavage sites and rho-independent transcription terminators. Furthermore, the absence of the restriction enzyme slicing sites (BmtI and HindIII) in the optimized nucleotide sequence was

confirmed. Next, the optimized sequence's N and C-terminals were supplemented with HindIII and BmtI restriction sites, respectively. Finally, using the limited cloning module in the SnapGene 3.2.1 program, the optimized adopted codon sequence of the vaccine construct was cloned into the *E. coli strain* pET28a (+) vector (Larentis *et al.*, 2011).

Final subunit vaccine immune simulation: A crucial step in researching the immune system is assessing the vaccine protein's possible immunogenicity and immune response profile by immunological simulation (Rosenberg and Sauna, 2018). Using the agent-based immune server C-ImmSim (https://kraken.iac.rm.cnr.it/C-IMMSIM/), the immunological simulation of the vaccine protein was carried out (Saha *et al.*, 2022). Using a position-specific scoring matrix (PSSM) and machine learning techniques, the C-ImmSim server predicts immunological interactions of epitopes (Manocha *et al.*, 2024). A minimum of four weeks should elapse between doses for the majority of vaccinations now in circulation. For the best possible product profile of a prophylactic onchocerciasis vaccine, the TOVA technique also recommends giving three shots spaced four weeks apart (Pineda *et al.*, 2008). For this reason, the simulation was run with the following default settings: The A MHC Class I A0101 allele, B MHC Class I B0702, and DR MHC Class II DRB1_0101 alleles that make up the host HLA selection, random seed 12345, simulation steps 100, simulation volume 10, and injection time step set to 1. Described as an antigen, C-ImmSim seeks to measure the immunological response that the immunization elicits in host cells human cells specifically after it is administered. In addition to measuring interferons, cytokines, and antibodies against the vaccine, the instrument can assess the amounts of helper T-cell 1 (Th1) and helper T-cell 2 (Th2) in the immune system. All things considered, this server aids in vaccine characterization and potential host immunological reactions.

Normal mode analysis of the complex: The iMODS online server accessible at (https://imods.iqf.csic.es/) is used to determine the atomic motions over an extended period of time within the vaccine-TLR7 complex (López-Blanco *et al.*, 2014). The MD simulation clarifies the complex's stability and structural dynamics (Pérez *et al.*, 2012).

The molecular dynamics (MD) of the vaccine-TLR7 complex: Gromax was used to simulate molecular dynamics (MD) of the vaccine-TLR7 complex. The procedure is separated into two stages: energy minimization, mild heating, and equilibration. After equilibration, a 20-ns simulation was run. To investigate post-simulation trajectories, we used Gromax during a 20-ns period.

RESULTS AND DISCUSSION: Protein sequence retrieval: By stimulating robust and long-lasting immune responses to certain pathogens or antigens, vaccines can stop infectious disease transmission, safeguarding both public and personal health (Doerr and Berger, 2014). To this aim, this study explored possible vaccine candidate using two *GTOV* proteins. These proteins were obtained in FASTA format from the NCBI database and included the nucleoprotein and nucleo-capsid protein.

The CTL specific epitopes prediction: It takes the engagement of CTL cells to successfully eradicate infections and establish durable immunity, including humoral immunity. As such, we fed the nucleo-capsid and nucleoprotein sequences to the NetCTL 1.2 server in order to predict CTL epitopes that would be immunogenic. A single 9-mer candidate was selected for vaccine development from among the predicted epitopes, based on their projected scores and strong MHC binding affinity (table 1).

NO	Proteins	Peptide sequence	Affinity	Affinity rescale	Cleavage	Tap	Combine score	Immunogenicity
1	Nucleoprotein	PTDPVELAV	0.2756	1.1703	0.9269	0.5080	1.2839	0.14399

Table 1: A selection of CTL epitopes. Each epitope is selected according to its score.

Helper T cells prediction: B cells are activated again, the immune response is regulated, and helper T cells promote the manufacture of antibodies. Th1 cells support cell-mediated immunity, while Th2 cells support humoral immunity. They can develop into a variety of subgroups, each with unique functions (Dobrzanski, 2013). The IEDB server received the protein sequences of nucleoprotein and nucleo-capsid in order to predict highly immunogenic epitopes. Non-overlapping sequence criteria and percentile ratings were used to select eight 15-mer HTL epitopes for the vaccine's development. Provided in table 2 are the chosen HTL epitopes.

No	Protein	Alleles	Start	End	Length	Core peptide	Peptide	Score	Rank
1	Nucleoprotein	HLA-DRB1*07:01	310	324	15	YIGSRSQII	EGWPYIGSRSQIIGR	0.971	0.04
2	---	HLA-DRB4*01:01	446	460	15	ITVQGADDI	QNSVITVQGADDIKK	0.7767	0.19
3	---	HLA-DRB1*03:01	283	297	15	MFIDERPGN	REGMFIDERPGNRNP	0.9057	0.33
4	---	HLA-DRB4*01:01	445	459	15	ITVQGADDI	PQNSVITVQGADDIK	0.6181	0.43
5	Nucleo-capsid Protein	HLA-DRB1*07:01	310	324	15	YIGSRSQIL	EGWPYIGSRSQILGR	0.9531	0.06
6	---	HLA-DRB1*03:01	283	297	15	MFIDERPGN	REGMFIDERPGNRNP	0.9057	0.33
7	---	HLA-DRB5*01:01	270	284	15	VKAALNVKR	FSSIVKAALNVKRRE	0.5722	0.68
8	---	HLA-DRB4*01:01	34	48	15	LIADSLDFT	DAKLIADSLDFTQVS	0.4196	1.1

Table 2: A list of carefully chosen HTL epitopes, chosen according to their percentile rank

Evaluation of B-cell epitopes: Antibodies are produced by B-Cells and are critical for both innate and immune responses. Because B-cell epitopes can initiate a variety of defensive mechanisms, such as cell-mediated cytotoxicity, complement system activation, neutralization, and agglutination, their proper design is crucial (Achkar *et al.*, 2015). The development of vaccine and therapies that effectively prevent *GTOV* infections depends on the selection of suitable B-cell epitopes. Consequently, four 16-mer epitopes were chosen for the creation of a vaccine after B-cell epitopes were found using the ABCpred service (table 3).

Protein	Rank	Sequence	Start position	Score
Nucleoprotein	2	WMDIEGPPTDPVELAV	414	0.90
---	4	HNGVIVPKKKNKEANS	536	0.85
Nucleo-capsid Protein	2	WMDIEGPPTDPVELAV	420	0.90
---	5	HNGVIVPKKKNKEANS	542	0.85

Table 3: Predicted linear B-cell epitopes are indicated along with the matching score

Final multi-epitope base vaccine design: In the context of vaccine development, short amino acid sequences known as linkers are used to join together different segments of the protein or peptide. Linkers are important in determining the vaccine's capacity to elicit an immune response, as well as its stability and efficacy (Tarrahimofrad *et al.*, 2021). KK and GPGPG linkers are used in the design of vaccines; thus, to create a multi-epitope subunit vaccine, we joined the epitopes of CTL, HTL, and B-cells using KK and GPGPG linkers (Basmenj *et al.*, 2023). In addition, we included HUMAN Beta-defensin 103, this can elicit immunological responses specific to antigens and is necessary for innate immunity, to increase the vaccine's ability to trigger an immunological response (Guryanova and Ovchinnikova, 2022). The HUMAN Beta-defensin 103 was linked to the N-terminal end of across the EAAAK linker of the vaccine sequence (figure 2).

Assessing the antigenic qualities, allergic potential, toxicity

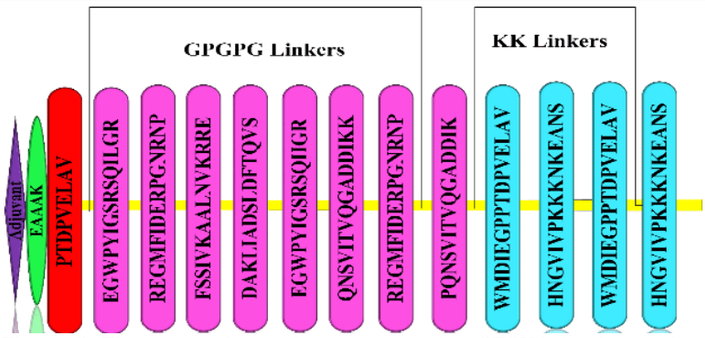

Figure 2: Final subunit vaccine construct for *GTOV* infection which include Human Beta-defensin 103, EAAAK linker, CTL, HTL, and B-cell epitopes with suitable linkers.

profile, and immunological response of the multi-epitope vaccine: The produced vaccine was tested for toxicity, allergic potential, and antigenic and immunogenic qualities. The immunogenicity was -0.22436, and the antigenicity is predicted by the ANTIGENpro server the score was 0.929968. Although the vaccine's antigenicity score of 0.6006 is predicted by the VaxiJen v2.0 service using the threshold value 0.4 Notably, the vaccine turned out to be non-allergic and non-toxic.

Examining the final vaccine product's physiochemical characteristics and solubility kinetics: The subunit vaccine construct's scaled solubility was estimated to be 0.7951 using the SoluProt server. The vaccine's physicochemical properties, the following parameters were examined: molecular weight, aliphatic index, theoretical isoelectric point (pI), half-life in *Escherichia coli*, amino acid concentration, and GRAVY value. The vaccine's molecular weight was found to be 33441.50. Its stability was demonstrated by its instability index of 37.16 (Naveed *et al.*, 2022), and its aliphatic index of 70.67 indicated significant thermos-stability (Firmansyah *et al.*, 2024). In *E. coli* the immunization had a half-life of more than 10 hours, indicating steady expression and simple purification in the bacterium (Huang *et al.*, 2012). 9.73 was recorded as the theoretical pI (Rafi *et al.*, 2023). A hydrophilic interaction with water was suggested by the GRAVY score of -0.613. Based on its physical features, the vaccine exhibits robust expression in *E. coli*, high thermos-stability, and simple purification (Chand and Singh, 2021). Our results align with earlier investigations on physicochemical properties.

Analysing the secondary structure of the final vaccine: The PSIPRED server was utilized in the construction of the vaccine's secondary structure (Abdollahi *et al.*, 2021). Figure 3 provides a graphic representation of the secondary structural components. In contrast to the 12.46% alpha-helix, 28.75% extended strand, 54.31% random coil, and 4.47% beta turn observed in this study, the vaccine is stable, as indicated by the instability index value of 37.16 Using expasy ProtParam tool (Ghosh *et al.*, 2019).

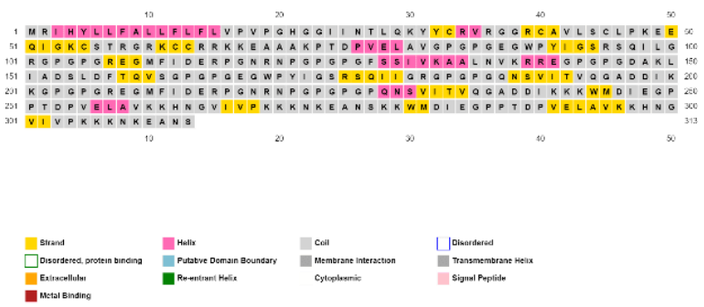

Figure 3: A picture that depicts the secondary structure of the vaccine. Pink hues characterize the helix, yellow-coloured beta-strand, and grey-coloured coil.

Vaccine's tertiary structure: To assist the immune system in identifying and responding to the infection, vaccines are formulated in a way that closely resembles the structure of the virus or bacterium they are intended to combat (Ogra *et al.*, 2001). To fabricate three-dimensional configurations for the vaccine design, the Robetta online platform was utilized, with the comparative modelling technique (Vishwakarma *et al.*, 2022). A thorough quality assessment was used to select the best model from the five prototypes that the Robetta server created for the vaccine design.

Improvement of the three-dimensional configuration of the vaccine: After the protein model was refined to perfection, the Galaxy Refine web server was utilized to improve its quality. Reducing energy usage and improving loops allowed for the remarkable quality of the intended construction to be realized. The original 'raw' vaccine model was refined using the Galaxy Refine web server, yielding five model structures altogether (Ashfaq *et al.*, 2021). When measured by a number of factors, Model 1 was shown to have a higher level of structural quality than the other structures. The MolProbity score 1.625, RMSD 0.292, and GDT-HA 0.9848 were among the many considerations made during the refinement process. The scores for clash and poor rotamer were determined to be 7.8 and 0.8, respectively, whereas the predicted Rama preferred score was 96.8 %.

Validation of the improved vaccine's three-dimensional configuration: An examination of Ramachandran plots was used to validate the improved model. The results showed that the Rama-favoured region contained 89% of the residues, whereas the additional allowed regions contained 9.6%, the generously allowed region contained 0.4%, and the forbidden region contained 0.9%, Figure 4B. Furthermore, the general quality and defects of the original 3D model were evaluated using the ERRAT and ProSA-web servers (Pradeepkiran *et al.*, 2021). The improved model. Figure 4A, had a Z-score of -4.8 according to ProSA-web, which is outside of the usual range for native proteins of the same size. Nevertheless, it is consistent with structures that have been verified through experiments and is close to the average value in the database. With the use of ERRAT, the improved model produced a 97.368% total quality factor, (figure 4C & 5).

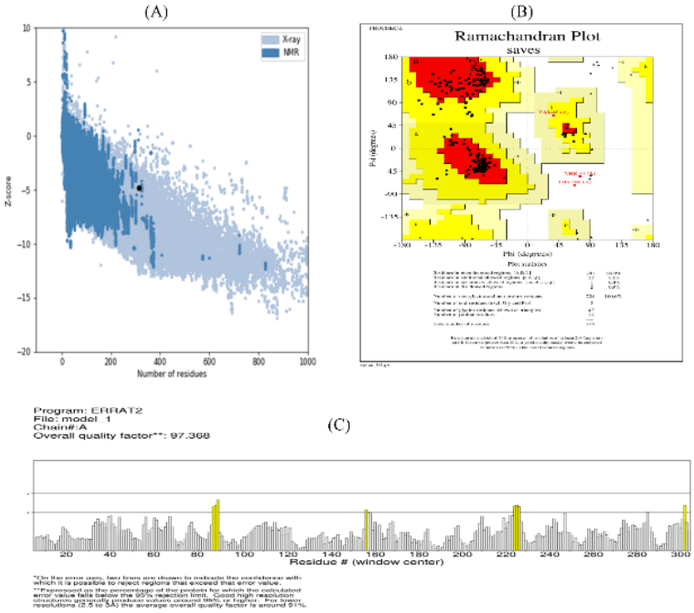

Figure 4: (A) The vaccine design's Z-score is shown by the black dot in the Z-score graph. (B) *GTOV* ramachandran graphic shows how torsional angles and. (C) using ERRAT to validate, showing the overall quality metric.

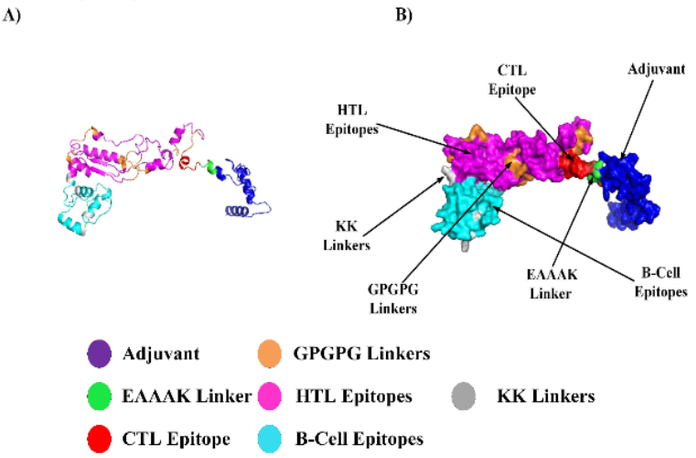

Figure 5: The 3D projected arrangement of the vaccine construct was visualized using PyMol and (A) multi-epitope vaccine in cartoon while (B) show the vaccine construct in surface view.

Forecasts for B-cell discontinuous epitopes: Furthermore, new conformational B-cell epitopes may arise from the structure and folding of a novel protein, requiring further predictions. With the ElliPro server, we were able to determine the discontinuous B-cell epitopes in the revised 3D model. 165 residues comprise the six new discontinuous B-cell epitopes that ElliPro predicted; scores ranged

from 27 to 63, (table 4 & figure 6).

No.	Residues	Number of residues	Score
1	A:M1, A:I3, A:H4, A:Y5, A:L6, A:L7, A:F8, A:A9, A:L10, A:L11, A:F12, A:L13, A:F14, A:L15, A:V16, A:P17, A:V18, A:P19, A:G20, A:H21, A:G22, A:G23, A:I24, A:I25, A:N26, A:T27, A:L28, A:Q29, A:K30, A:Y31, A:Y32, A:C33, A:R34, A:V35, A:R36, A:G37, A:G38, A:R39, A:C40, A:A41, A:V42, A:L43, A:S44, A:C45, A:L46, A:P47, A:K48, A:E49, A:E50, A:Q51, A:I52, A:G53, A:K54, A:C55, A:S56, A:T57, A:R58, A:G59, A:R60, A:K61, A:C62, A:C63, A:K66	63	0.812
2	A:M245, A:D246, A:I247, A:E248, A:G249, A:P250, A:P251, A:T252, A:D253, A:K260, A:N263, A:G264, A:V265, A:I266, A:V267, A:P268, A:K269, A:K270, A:K271, A:N272, A:K273, A:E274, A:A275, A:N276, A:S277, A:K278, A:K279, A:W280, A:P287, A:D289, A:E292, A:L293, A:A294, A:V295, A:K296, A:K297, A:H298, A:N299, A:G300, A:V301, A:I302, A:V303, A:P304, A:K306, A:N312, A:S313	46	0.711
3	A:D282, A:I283, A:E284, A:G285	4	0.661
4	A:N136, A:R139, A:R140	3	0.633
5	A:G82, A:P83, A:G84, A:P85, A:G86, A:E87, A:G88, A:W89, A:P90, A:Y91, A:I92, A:G93, A:S94, A:S96, A:Q97, A:I98, A:G100, A:R101, A:G102, A:G104, A:P105, A:G106	22	0.606
6	A:E141, A:G142, A:P143, A:G144, A:P145, A:G146, A:G195, A:A196, A:D197, A:D198, A:K200, A:K201, A:G202, A:P203, A:G204, A:P205, A:G206, A:R207, A:E208, A:G209, A:M210, A:F211, A:I212, A:G236, A:A237, A:D238, A:K242	27	0.562

Table 4: The scores assigned to the anticipated B-cell discontinuous epitopes.

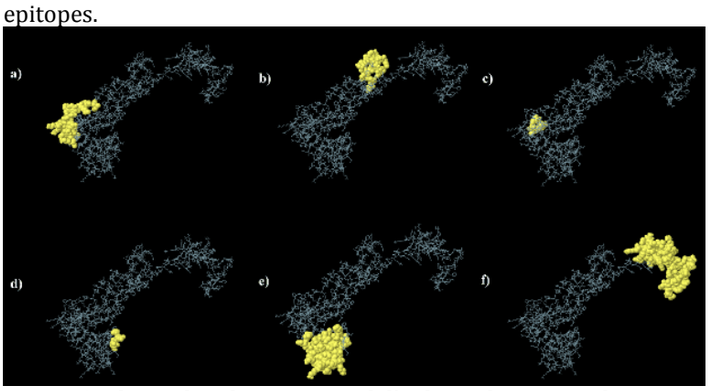

Figure 6: The updated vaccine model's three-dimensional versions of the six predicted discontinuous B-cell epitopes.

Molecular docking with TLR7: Immune receptors and antigen molecules must be correctly linked in order to initiate an immune response. This was accomplished by creating a subunit vaccine and using the HDOCK server to dock it with the human immunological receptor TLR7. TLR7 have the ability to efficiently initiate an immune response subsequent to the identification of a virus. Strong interactions were found between TLR7 and the vaccine construct according to the docking study. TLR7 had binding values that were -317.72 Kcal/mol. Using PyMOL, the vaccine and TLR7 complex were visualized following the docking analysis (figure 7A). The vaccination and TLR7 combination exhibited 211 non-bonding contacts, 14 hydrogen bonds, and 3 salt bridges when the docked complex was subjected to further analysis using the PDBsum website to assess the protein-protein interactions (figure 7B & 7C).

An examination of papulation coverage: A thorough population distribution analysis was conducted on the identified HTL vaccine

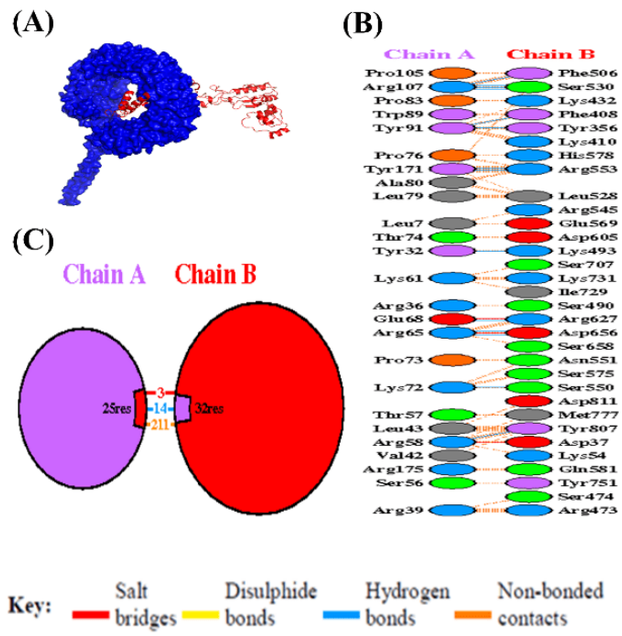

Figure 7: (A) The geometry of vaccine binding with TLR7. (B–C) interaction of the vaccine TLR7 complex with other proteins and receptor molecule is indicated by Chain A, while a vaccine molecule is indicated by Chain B.

candidates and the matching HLA alleles. The analysis revealed that there was excellent population coverage worldwide. The number of epitope hits and HLA combinations identified was 0, 1, 2, 3, and 4. The percentage of each individual population was 65.72, 0.0, 32.49, 0.0, 1.79, and the cumulative population coverage percentage was 100.0, 34.28, 34.28, 1.79, 1.79 Table 5. The world is appropriately and extensively dispersed with HTL-cell vaccine possibilities. A population coverage analysis is displayed in (figure 8 & table 6).

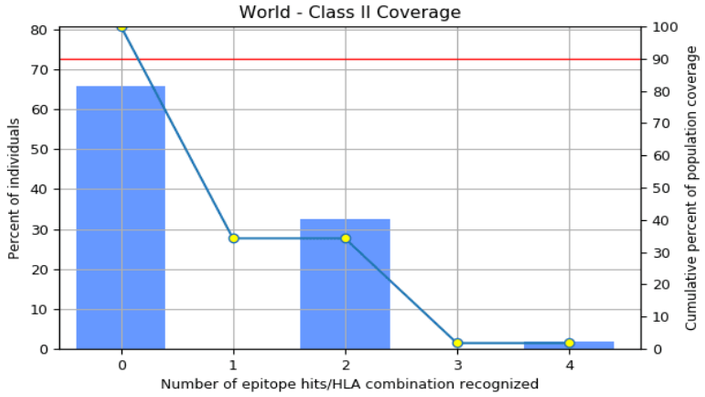

Figure 8: Analysis of the MHC Class 2 restricted epitopes' population coverage derived from nucleo-capsid and nucleoprotein.

The vaccine construct's *in-silico* cloning: To convert the protein in the vaccine back into a nucleotide sequence, the EMBOSS tool was employed. After that, the JCat tool was applied to the reversed sequence. With the Java codon adaptation tool, one may determine the optimal GC content percentage and codon adaptation index (CAI) value to get significant levels of protein production. The codon use of the vaccine antigen gene is assumed to have been adjusted to match that of the host organism. The gene will thus likely express itself more successfully in such scenario, leading to an increase in the manufacture of antigens and maybe a more potent vaccine. The *GTOV* vaccine's estimated percentage of GC content in this study was 53.35%. Remarkably, it has been shown that in the *E. Coli K12 strain*, a GC content of greater than 50% increases the viral sequence expression rate. This sequence produced a computed CAI value of 0.95. Thirty to seventy percent is the recommended range for GC content, and a score of more than 0.8 on the CAI is usually considered good (Kizhakedathil *et al.*, 2024). According to other studies that discovered similar data ranges for sustained vaccine expression, (Girard *et al.*, 2005), our results show the high rates of expression of the planned vaccine. Using the restriction enzymes HindIII and Bmti, we finally cloned the optimized *GTOV* sequence into the pET28a (+) vector, (figure 9).

Immune simulation of the vaccine: The development of vaccines requires immune simulation. Without actually causing disease, a vaccination seeks to stimulate the body's immune system to defend

against a particular virus (Germain, 2010).

Epitope	Coverage	HLA (genotypic frequency (%)) allele				Total HLA hits
	Class II	HLA-DRB1*03:01 (10.47)	HLA-DRB1*07:01 (10.71)	HLA-DRB4*01:01 (0.0)	HLA-DRB5*01:01 (0.0)	
Epitope #1: EGWPYIGSRSQILGR	18.23%	Negative	Positive	Negative	Negative	1
Epitope #2: REGMFIDERPGNRNP	17.84%	Positive	Negative	Negative	Negative	1
Epitope #3: FSSIVKAALNVKRRE	0.0	Negative	Negative	Negative	Positive	1
Epitope #4: DAKLIADSLDFTQVS	0.0	Negative	Negative	Negative	Negative	1
Epitope #5: EGWPYIGSRSQIIGR	18.23%	Negative	Negative	Negative	Negative	1
Epitope #6: QNSVITVQGADDIKK	0.0	Negative	Negative	Positive	Negative	1
Epitope #7: REGMFIDERPGNRNP	17.84%	Positive	Negative	Negative	Negative	1
Epitope #8: PQNSVITVQGADDIK	0.0	Negative	Negative	Positive	Negative	1
Epitope set	34.28%	2	2	3	1	8

Table 6: Coverage of individual epitope in the world.

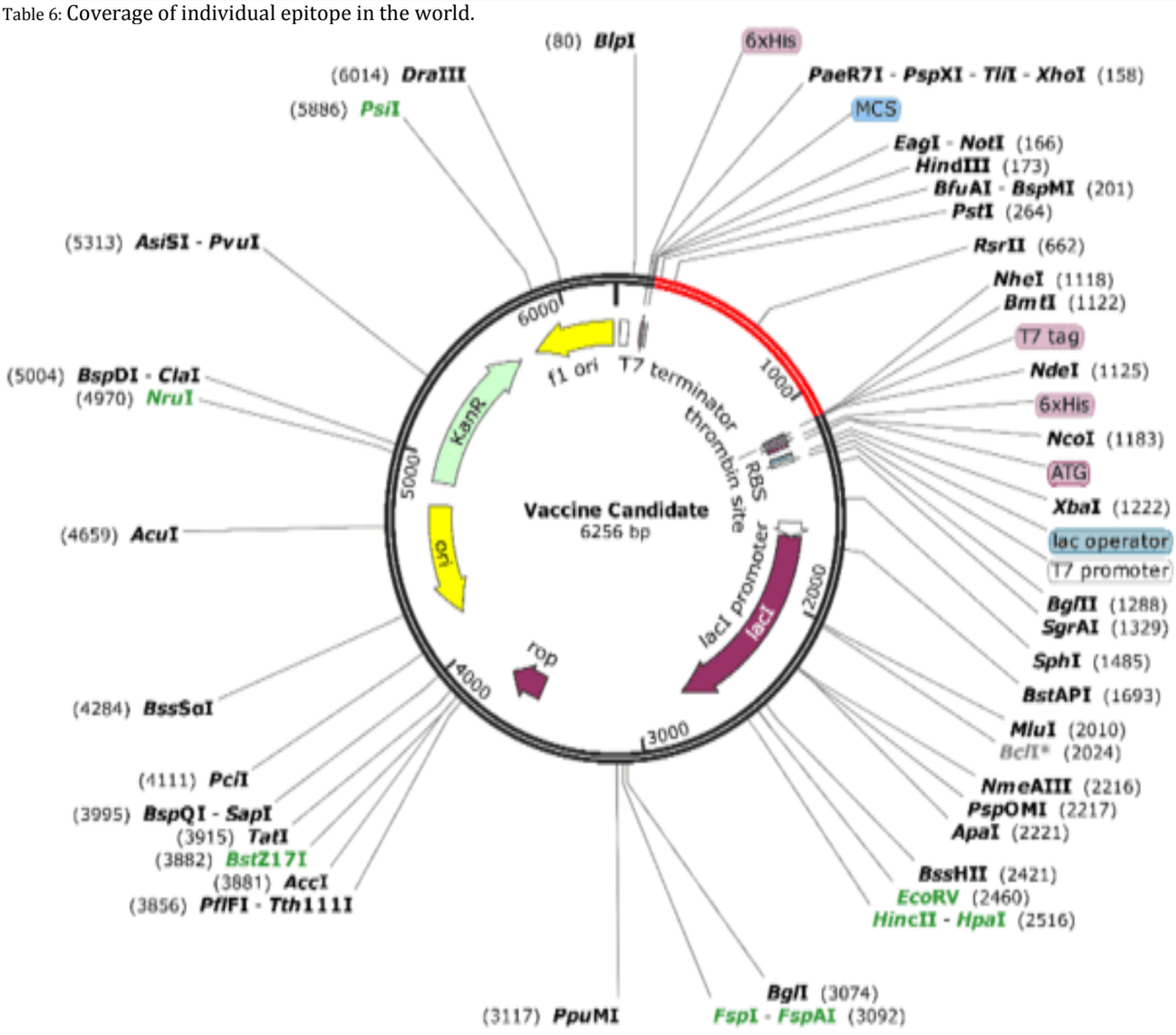

Figure 9: The *in-silico* cloning of the constructed vaccine in pET28a (+) vector the cloned sequence of the vaccine is shown in the red colour.

Consequently, we used the C-ImmSim server to run immunological simulations in order to evaluate the immunological reaction that our manufactured vaccine have caused. Following vaccine, significant primary immune responses were observed. IgM antibodies have a titer scale larger than 400000/mL, whereas IgM+IgG antibodies have a titer scale closer to 600000/mL, as illustrated in, (figure 10A).

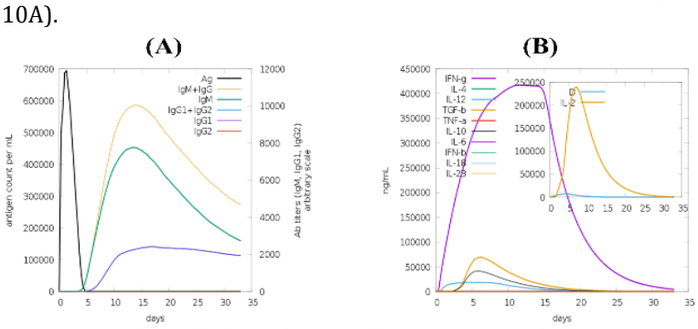

Figure 10: (A) Black indicates the injection of the antigenic component; other colours show the immune responses that the vaccine elicits and (B) the amounts of cytokines and interleukins in response to the *GTOV* vaccine.

High titter scales of approximately 140000/mL and 150000/ml, respectively, were achieved by IgG1+IgG2 and IgG1. It was discovered that the IgG2 antibody response persisted in being negligible throughout the postnatal phase. Cytokines and interleukins have a major role in promoting the immune response that vaccine induce. Once immunized, the vaccine antigen is recognized by the immune system's antigen-presenting cells (APCs), which prepare it for release to T cells (Donnelly *et al.*, 2000). T Cells are activated by this process, and they release cytokines like IL-2 and interferon-gamma (IFN-γ) that help B Cells and T Cells proliferate and differentiate. Vaccine-targeted pathogens can be neutralized by antibodies produced by B cells (Shukla *et al.*, 2021). Following vaccine, Interleukins (IL), and Cytokines increased significantly. Following a gradual increase, the IFN-g levels for the intended vaccine approached is 430,000/ml. Similarly, there was a greater concentration of IL-2, nearly 250,000/ml, Figure 10B. As a result, our vaccine against *GTOV* showed a higher level of immunogenicity since it was competent to evoke a strong immune response.

Vaccine-TLR7 Normal mode simulation: The dynamics and stability of the vaccine TLR7 docked complex were examined using

normal mode simulations run on the iMODS server (figure 11). A deformability graph was made in order to assess a molecule's deformability at each residue for the first time. It was predicted that the NMA and B-factor tests would be modified in the future. The model relative stiffness was shown by the eigenvalue plot that was subsequently developed, where simpler deformations were associated with lower eigenvalue. The eigenvalue was determined to be 2.853256e-06.

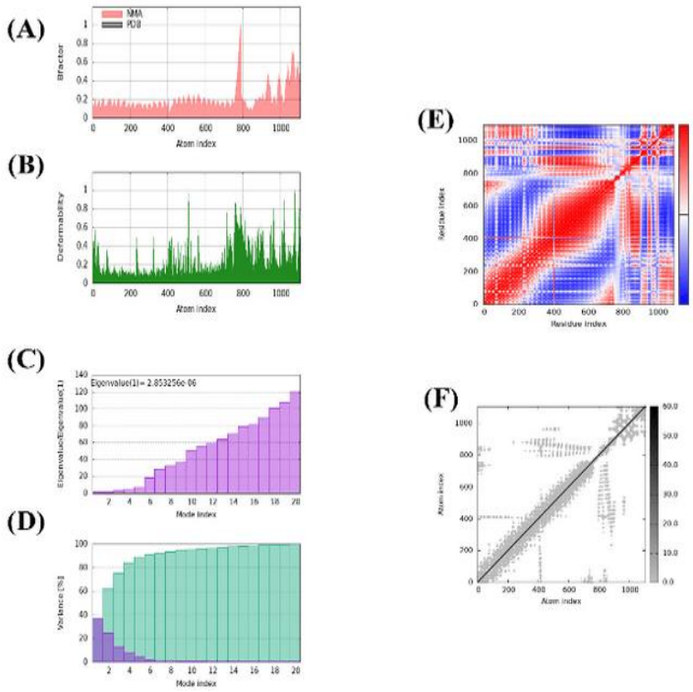

Figure 11: Normal mode simulation of docked vaccine TLR7, (A) NMA and experimental B-factor, (B) molecular volume at each residual deformability, (C) eigenvalue plot showing protein stiffness, (D) variance (E) correlated (red) and anti-correlated (blue) paths, and (F) elastic network diagram.

The generated variance graph shows the inverse relationship between the variance and eigenvalue of each normal mode. The macromolecules segments exhibit three distinct motion pattern: uncorrelated white, correlated red, and anti-correlated blue are displayed on the co-variance map. The atom to atom connection's stiffness was displayed on the elastic network graph; stiffer springs were indicating by darker colour.

Simulated TLR7-vaccine complex using MD: We used molecular dynamics simulations to study the stability and volatility of the TLR-7 complex and vaccine design. Figure 12 showed the computed RMSD and RMSF for the protein, side chains, and vaccine, along with the corresponding graphs. After 20 ns of simulation, the TLR-7 vaccine's system stability was tested for residue and side chain with an overall RMSD rate of 0-8Å. The RMSF of the system's highest residue was also satisfactory, however certain residues were more volatile. The RoG analysis reveals that the protein structure remained compact throughout the MD simulations. Figure 12C shows that RoG began at 68.55, fell to 68.45, rebounded to 68.55, and finally reached 68.40 at the end of the track.

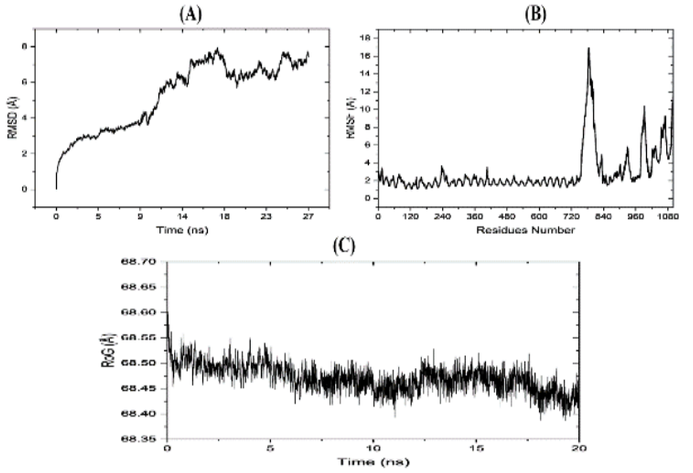

Figure 12: MD simulation of vaccine-TLR7 complex. (A) RMSD plot of the vaccine-TLR7 complex. (B) RMSF plot of the vaccine-TLR7 complex and (C) RoG diagram of the vaccine-TLR7 complex.

It was discovered that the *GTOV* proteins, such as nucleo-capsid and nucleoprotein, are antigenic and essential for infection and host-replication. They are therefore regarded as being crucial for the investigation of subunit vaccines. A widely accepted strategy for eliminating or controlling the infection is immunization or vaccination. Subunit vaccine design entered a new era with the development of computer methods and their applications to biological research, wherein Instead of using the full pathogen as a tool for vaccination, the most precise or accurate antigenic portion is found. By far the most common and efficient method in the creation of small molecule inhibitors and vaccine candidates using computer algorithms (Guarra and Colombo, 2023). Rapid collection of extensive pathogen genomic and proteome data, such as *GTOV*, aids in the creation of efficient vaccine based on epitopes that are used to prevent and treat diseases brought on by a variety of illnesses. Using viral proteins as a basis, computational methods identified epitopes (CTL & HTL), and validation scores of these epitopes indicate their potential utility in the development of subunit vaccines. Major Histocompatibility Complexes (MHCs) come in several forms. MHC-I transports a 9-mer peptide to the cell's surface where it functions as an impulsive signal for cytotoxic T cells, which demolish cells by initiating a complementary immunological cascade. Helper T cells receive a 15-mer peptide from MHC-II molecules. High-affinity CTL, B-cell, and HTL epitopes are combined in our final subunit vaccine to induce immunity. The vaccine's allergenicity and antigenicity values were determined; these values show that the vaccine is not allergenic and that its antigenic nature may elicit an immune response.

Together with these epitopes, we also predict linear B-Cell epitopes, which aid in B-cell maturation and antibody production. Calculations were made to determine the thermal stability, aliphatic array, molecular weight, and theoretical pI of vaccine. The vaccine has a molecular weight of 33441.50 kDa, which is within the acceptable range for a subunit vaccine. Its theoretical pI score of 9.73 suggests that the vaccine is fundamental in nature. The vaccine's thermal stability is supported by the instability index, and the aliphatic array implies that the vaccine contains aliphatic side chains. The vaccine's secondary structure was predicted and analysed using the Sopma Secondary Structure Prediction Server, which shows that it has 12.46% alpha-helix, 28.75% extended strand, Random Coil 54.31%, and 4.47% beta turn. The 3D structure that is produced by homology modelling also provides valuable assistance for studying the normal function, dynamics, and interactions of proteins with ligands and other proteins, in addition to providing adequate detail regarding the special configuration of these crucial protein residues. Several structural validation techniques were utilized to identify faults in the final 3D structure of the vaccine. Based on the primary Ramachandran plot, it was determined that the complete model is acceptable since the majority of residues were located in the most-favourable zone and a small number were found in disorder area. Additionally, the vaccine was TLR7 docked in order to comprehend the immunological response to the final vaccine composition. To keep the overall system potential energy for the structural stability of the docked vaccine protein-TLR7, as low as possible, energy minimization was carried out. A more comparatively stable structure with appropriate stereochemistry is generated as a result of energy minimization, which fixes the structure's superfluous topology by removing some protein atoms.

The goal of codon optimization using CAI (Codon Adaptation Index) was to achieve maximal expression in terms of translation and transcription of the vaccine protein in the host *E. coli* strain k-12. A critical prerequisite for many biochemical processes is the recombinant protein's overexpression solubility in the host *E. coli*. An acceptable amount of solubility in the host is exhibited by our vaccine protein. The main objective of several mechanical and biological applications is to fortify the protein. This work used contemporary immune-informatics techniques to create novel, affordable, and efficient subunit vaccine to combat *GTOV*. This vaccine is risk-free and immunogenic, utilizing the body's defences against *GTOV* infection. A VaxiJen v2.0 vaccine's antigenicity score of 0.6006 was obtained while the antigenicity score of the vaccine is obtained from the ANTIGENpro server was 0.929968 in this investigation. According to the instability index value of 37.16, means that the vaccine is stable. As opposed to the 12.46% alpha-helix, 28.75% prolonged strand, 54.31% random coil, and 4.47%

beta turn found in this vaccine construct. A larger percentage of coil indicates an easier time for denaturing. Protein expression and purification depend heavily on the half-life. We discovered that the vaccine had half-lives of 10, 20, and 30in human, *yeast,* and *E. coli* systems, respectively. These increased half-lives suggest that more frequent immunizations could be helpful, potentially increasing immune responses. TLR 7 was utilized in this investigation. In this investigation, the reported CAI value is 0.95. This likely indicates the strength of the vaccine design. Using iMODS normal mode simulations, the stability of the complex was evaluated by examining many components, including the elastic network, deformability, B-factor, and residue dynamics. The result demonstrates the vaccine-TLR7 combination's flexibility and stability. The efficacy of the multi-epitope vaccine (MEV) in inducing humoral, innate, and cellular immune response has been shown by immunological simulation.

CONCLUSION: Due to the antigenic nature of the two proteins used in this study, the primary goal was to use *in-silico* methods to create an efficient multi-epitope vaccination against the *GTOV*. B, cytotoxic T, and Helper T cell epitopes were predicted in order to create a vaccine since MHC-I and II presents the pathogen epitope. To fuse these epitopes, appropriate linkers were employed. To guarantee the vaccine's efficacy, the tertiary structure was anticipated and verified. Stability, allergenicity, and antigenicity were calculated among the physicochemical characteristics. In order to determine the vaccine's affinity for the receptor, TLR-7 was docked with it. In order to achieve maximum expression of the vaccine in the host (*E. coli*), the protein was reverse-translated for codon adaptation. This study can aid in the control of *GTOV* infection; however, an experimental validation in a wet lab is required to ensure the vaccine design's activity.

FUNDING: This research was conducted without any funding.

CONFLICT OF INTEREST: The authors declare that the research was conducted in the absence of any commercial or financial relationships that could be construed as a potential conflict of interest.

LIFE SCIENCE REPORTING: In current research article no life science threat was reported.

ETHICAL RESPONSIBILITY: This is original research, and it is not submitted in whole or in parts to another journal for publication purpose.

INFORMED CONSENT: The author(s) have reviewed the entire manuscript and approved the final version before submission.

REFERENCES:

Abbott, R. K. and S. Crotty, 2020. Factors in b cell competition and immunodominance. Immunological reviews, 296(1): 120-131.

Abdollahi, S., Z. Raoufi and M. H. Fakoor, 2021. Physicochemical and structural characterization, epitope mapping and vaccine potential investigation of a new protein containing tetratrico peptide repeats of acinetobacter baumannii: An in-silico and in-vivo approach. Molecular immunology, 140: 22-34.

Abraham Peele, K., T. Srihansa, S. Krupanidhi, V. S. Ayyagari and T. Venkateswarulu, 2021. Design of multi-epitope vaccine candidate against sars-cov-2: A in-silico study. Journal of biomolecular structure and dynamics, 39(10): 3793-3801.

Achkar, J. M., J. Chan and A. Casadevall, 2015. Role of b cells and antibodies in acquired immunity against mycobacterium tuberculosis. Cold spring harbor perspectives in medicine, 5(3): a018432.

Ahmad, S., F. M. Demneh, B. Rehman, T. N. Almanaa, N. Akhtar, H. Pazoki-Toroudi, A. Shojaeian, M. Ghatrehsamani and S. Sanami, 2024. In silico design of a novel multi-epitope vaccine against hcv infection through immunoinformatics approaches. International journal of biological macromolecules, 267: 131517.

Alberts, B., A. Johnson, J. Lewis, M. Raff, K. Roberts and P. Walter, 2002. Protein function. In: Molecular biology of the cell 4th edition. Garland science.

Almofti, Y. A., K. A. Abd-Elrahman and E. E. Eltilib, 2021. Vaccinomic approach for novel multi epitopes vaccine against severe acute respiratory syndrome coronavirus-2 (sars-cov-2). BMC immunology, 22: 1-20.

Ashfaq, U. A., S. Saleem, M. S. Masoud, M. Ahmad, N. Nahid, R. Bhatti, A. Almatroudi and M. Khurshid, 2021. Rational design of multi epitope-based subunit vaccine by exploring mers-cov proteome: Reverse vaccinology and molecular docking approach. PLoS One, 16(2): e0245072.

Bachmann, M. F. and G. T. Jennings, 2010. Vaccine delivery: A matter of size, geometry, kinetics and molecular patterns. Nature reviews immunology, 10(11): 787-796.

Barreto, S. M., R. B. Barata and G. L. Werneck, 2024. Epidemiological challenges in latin america and the caribbean. In: Handbook of epidemiology. Springer: pp: 1-52.

Basmenj, E. R., M. Arastonejad, M. Mamizadeh, M. Alem, M. KhalatbariLimaki, S. Ghiabi, A. Khamesipour, H. Majidiani, M. Shams and H. Irannejad, 2023. Engineering and design of promising t-cell-based multi-epitope vaccine candidates against leishmaniasis. Scientific reports, 13(1): 19421.

Bell, D. M., E. W. Brink, J. L. Nitzkin, C. B. Hall, H. Wulff, I. D. Berkowitz, P. M. Feorino, R. C. Holman, C. L. Huntley and R. H. Meade III, 1981. Kawasaki syndrome: Description of 2 outbreaks in the united states. New england journal of medicine, 304(26): 1568-1575.

Bhagwat, P., A. Amobonye, S. Singh and S. Pillai, 2021. A comparative analysis of gh18 chitinases and their isoforms from beauveria bassiana: An in-silico approach. Process biochemistry, 100: 207-216.

Bhattacharjee, M., M. Banerjee and A. Mukherjee, 2023. In silico designing of a novel polyvalent multi-subunit peptide vaccine leveraging cross-immunity against human visceral and cutaneous leishmaniasis: An immunoinformatics-based approach. Journal of molecular modeling, 29(4): 99.

Blumberg, L., D. Enria and D. G. Bausch, 2014. Viral haemorrhagic fevers. In: Manson's tropical infectious diseases. WB Saunders: pp: 171-194. e172.

Camberlin, P., 2018. Climate of eastern africa. Oxford research encyclopedia of climate science.

Chand, Y. and S. Singh, 2021. Prioritization of potential vaccine candidates and designing a multiepitope-based subunit vaccine against multidrug-resistant salmonella typhi str. Ct18: A subtractive proteomics and immunoinformatics approach. Microbial Pathogenesis, 159: 105150.

Charrel, R. N., X. de Lamballerie and S. Emonet, 2008. Phylogeny of the genus arenavirus. Current opinion in microbiology, 11(4): 362-368.

Chung, B. K.-S. and D.-Y. Lee, 2012. Computational codon optimization of synthetic gene for protein expression. BMC systems biology, 6: 1-14.

Cline, C., X. Zeng, T. M. Bell, C. Shaia, P. Facemire, J. Williams, N. Davis, A. Babka, E. Picado and C. Fitzpatrick, 2023. Temporal changes in pathology and viral rna distribution in guinea pigs following separate infection with two new world arenaviruses. PLoS neglected tropical diseases, 17(9): e0011620.

Dobrzanski, M. J., 2013. Expanding roles for cd4 t cells and their subpopulations in tumor immunity and therapy. Frontiers in oncology, 3: 63.

Doerr, H. W. and A. Berger, 2014. Vaccination against infectious diseases: What is promising? Medical microbiology and immunology, 203: 365-371.

Donnelly, J. J., M. A. Liu and J. B. Ulmer, 2000. Antigen presentation and DNA vaccines. American journal of respiratory and critical care medicine, 162(supplement_3): S190-S193.

Doytchinova, I. A. and D. R. Flower, 2007. Vaxijen: A server for prediction of protective antigens, tumour antigens and subunit vaccines. BMC bioinformatics, 8: 1-7.

Dufour, V. M. A. S., 2021. Ecology of francisella tularensis in sympatric rodent and lagomorph species in urban and non-urban settings in prairie canada. University of Saskatchewan, Saskatoon, Canada.

Elumalai, A. and A. J. McKee, 2021. Biological agents. In: Mitigating mass violence and managing threats in contemporary society. IGI Global: pp: 195-211.

Enria, D. A., 2005. Arenaviral hemorrhagic fevers: Argentine hemorrhagic fever and lassa fever. Neurological disease and therapy, 67: 115.

Fadaka, A. O., N. R. S. Sibuyi, D. R. Martin, M. Goboza, A. Klein, A. M. Madiehe and M. Meyer, 2021. Immunoinformatics design of a novel epitope-based vaccine candidate against dengue virus. Scientific reports, 11(1): 19707.

Feisal, M. R., 2015. In silico structural analysis, physicochemical characterization and homology modeling of arabidopsis thaliana na+/h+ exchanger 1 protein. BRAC University.

Ferdous, S., S. Kelm, T. S. Baker, J. Shi and A. C. Martin, 2019. B-cell

epitopes: Discontinuity and conformational analysis. Molecular immunology, 114: 643-650.

Fernandes, J., A. Guterres, R. C. De Oliveira, J. Chamberlain, K. Lewandowski, B. R. Teixeira, T. A. Coelho, C. F. Crisóstomo, C. R. Bonvicino and P. S. D'Andrea, 2018. Xapuri virus, a novel mammarenavirus: Natural reassortment and increased diversity between new world viruses. Emerging microbes & infections, 7(1): 1-10.

Firmansyah, R. P., S. N. Alimah, I. M. Artika and P. A. Kurniatin, 2024. In silico phylogenetic, physicochemical, and structural characteristics of phytase enzyme from ten aspergillus species. Menara perkebunan, 92(1):11-13.

Gerken, K. N., A. D. LaBeaud, H. Mandi, M. L. A. Jackson, J. G. Breugelmans and C. H. King, 2021. Paving the way for human vaccination against rift valley fever virus: A systematic literature review of rvfv epidemiology from 1999 to 2021. MedRxiv: 2021.2009. 2029.21264307.

Germain, R. N., 2010. Vaccines and the future of human immunology. Immunity, 33(4): 441-450.

Ghani, A. C., C. A. Donnelly, D. R. Cox, J. Griffin, C. Fraser, T. Lam, L. Ho, W. Chan, R. Anderson and A. Hedley, 2005. Methods for estimating the case fatality ratio for a novel, emerging infectious disease. American journal of epidemiology, 162(5): 479-486.

Ghosh, R., A. Upadhyay, A. Roy and A. Tiwari, 2019. Structural and functional analysis of aquaporin protein of different fish species. Journal of entomology and zoological studies, 7: 94-107.

Girard, M. P., T. Cherian, Y. Pervikov and M. P. Kieny, 2005. A review of vaccine research and development: Human acute respiratory infections. Vaccine, 23(50): 5708-5724.

Guajira, L., 1995. Venezuelan equine encephalitis—colombia, 1995.

Guarra, F. and G. Colombo, 2023. Computational methods in immunology and vaccinology: Design and development of antibodies and immunogens. Journal of chemical theory and computation, 19(16): 5315-5333.

Guedes, I. A., C. S. de Magalhães and L. E. Dardenne, 2014. Receptor–ligand molecular docking. Biophysical reviews, 6: 75-87.

Guryanova, S. V. and T. V. Ovchinnikova, 2022. Immunomodulatory and allergenic properties of antimicrobial peptides. International journal of molecular sciences, 23(5): 2499.

Hayward, A. R., 2015. The experience of a nurse who survived a highly pathogenic novel arenavirus. Faculty of Health Sciences, University of the Witwatersrand, Johannesburg.

Hervé, C., B. Laupèze, G. Del Giudice, A. M. Didierlaurent and F. Tavares Da Silva, 2019. The how's and what's of vaccine reactogenicity. NPJ Vaccines, 4(1): 1-11.

Hozori, S., R. Rahimi and Z. Shekofteh, 2023. An immunoinformatics approach to design a potential multi-epitope subunit vaccine against bordetella pertussis. Informatics in medicine unlocked, 42: 101358.

Huang, C.-J., H. Lin and X. Yang, 2012. Industrial production of recombinant therapeutics in escherichia coli and its recent advancements. Journal of industrial microbiology and biotechnology, 39(3): 383-399.

Irsal, R. A. P., G. M. Gholam, M. A. Dwicesaria and F. Chairunisa, 2024. Computational investigation of y. Aloifolia variegate as anti-human immunodeficiency virus (hiv) targeting hiv-1 protease: A multiscale in-silico exploration. Pharmacological research-modern chinese medicine, 11: 100451.

Ismail, N. O., 2015. Functional characterization of a peptide fragment, os (3-12), derived from the carboxy-terminal region of a defensin from the tick ornithodoros savignyi. University of Pretoria (South Africa).

Kader, M. A., A. Ahammed, M. S. Khan, S. A. Al Ashik, M. S. Islam and M. U. Hossain, 2022. Hypothetical protein predicted to be tumor suppressor: A protein functional analysis. Genomics & informatics, 20(1).

Kahan, S., 2008. Signs and symptoms. Lippincott Williams & Wilkins.

Khan, S., S. S. Ali, I. Zaheer, S. Saleem, Ziaullah, N. Zaman, A. Iqbal, M. Suleman, A. Wadood and A. U. Rehman, 2022. Proteome-wide mapping and reverse vaccinology-based b and t cell multi-epitope subunit vaccine designing for immune response reinforcement against porphyromonas gingivalis. Journal of biomolecular structure and dynamics, 40(2): 833-847.

Kizhakedathil, M., M. Jain, S. Govindaraj, A. Sundararaju, K. Vijayakumar and T. Karuppusamy, 2024. Design of a chimeric vaccine targeting opa protein of neisseria gonorrhoeae–an immunoinformatics approach. Biointerface research applied chemistry, 14: 25.

Kizhakedathil, M. P. J., T. Saravanakumar, S. Anbarasu, S. Kallesh and V. Thiruvalluvan, 2022. Designing of chimeric vaccine against canine distemper virus targeting hemaglutanin protein. Biointerface research applied chemistry, 13: 347.

Kumar, P., P. Kumar, A. Shrivastava, M. A. Dar, K. B. Lokhande, N. Singh, A. Singh, R. Velayutham and D. Mandal, 2023. Immunoinformatics-based multi-epitope containing fused polypeptide vaccine design against visceral leishmaniasis with high immunogenicity and tlr binding. International journal of biological macromolecules, 253: 127567.

Larentis, A. L., A. P. C. Argondizzo, G. dos Santos Esteves, E. Jessouron, R. Galler and M. A. Medeiros, 2011. Cloning and optimization of induction conditions for mature psaa (pneumococcal surface adhesin a) expression in escherichia coli and recombinant protein stability during long-term storage. Protein expression and purification, 78(1): 38-47.

Larsen, M. V., C. Lundegaard, K. Lamberth, S. Buus, O. Lund and M. Nielsen, 2007. Large-scale validation of methods for cytotoxic t-lymphocyte epitope prediction. BMC bioinformatics, 8: 1-12.

Lendino, A., A. A. Castellanos, D. M. Pigott and B. A. Han, 2024. A review of emerging health threats from zoonotic new world mammarenaviruses. BMC microbiology, 24(1): 115.

Liang, C., E. Bencurova, E. Psota, P. Neurgaonkar, M. Prelog, C. Scheller and T. Dandekar, 2021. Population-predicted mhc class ii epitope presentation of sars-cov-2 structural proteins correlates to the case fatality rates of covid-19 in different countries. International journal of molecular sciences, 22(5): 2630.

López-Blanco, J. R., J. I. Aliaga, E. S. Quintana-Ortí and P. Chacón, 2014. Imods: Internal coordinates normal mode analysis server. Nucleic acids research, 42(W1): W271-W276.

Loyd, K. A. T., 2015. Sociopolitical, ecological and behavioural aspects of free-roaming cats. Unpublished PhD Thesis University of Georgia, Georgia Greece.

MacLachlan, B. J., G. Dolton, A. Papakyriakou, A. Greenshields-Watson, G. H. Mason, A. Schauenburg, M. Besneux, B. Szomolay, T. Elliott and A. K. Sewell, 2019. Human leukocyte antigen (hla) class ii peptide flanking residues tune the immunogenicity of a human tumor-derived epitope. Journal of biological chemistry, 294(52): 20246-20258.

Mahapatra, S. R., J. Dey, T. K. Raj, N. Misra and M. Suar, 2023. Designing a next-generation multiepitope-based vaccine against staphylococcus aureus using reverse vaccinology approaches. Pathogens, 12(3): 376.

Manocha, N., P. Kumar and M. Khanna, 2024. Immunoinformatic approach to design ctl epitope based chimeric vaccine targeting multiple serotypes of dengue virus. bioRxiv: 2024.2001. 2015.575641.

Manzione, N. d., R. A. Salas, H. Paredes, O. Godoy, L. Rojas, F. Araoz, C. F. Fulhorst, T. G. Ksiazek, J. N. Mills and B. A. Ellis, 1998. Venezuelan hemorrhagic fever: Clinical and epidemiological studies of 165 cases. Clinical infectious diseases, 26(2): 308-313.

Mao, B., R. Tejero, D. Baker and G. T. Montelione, 2014. Protein nmr structures refined with rosetta have higher accuracy relative to corresponding x-ray crystal structures. Journal of the american chemical society, 136(5): 1893-1906.

Matamoros-Recio, A., 2023. Check for updates chapter 1 modeling of transmembrane domain and full-length tlrs in membrane models alejandra matamoros-recio, marina mínguez-toral, and sonsoles martín-santamaría. Toll-like receptors: methods and protocols, 2700: 1.

Medina, M. G., 2022. Functional molecular motions in drug design: Application to nicotinic acetylcholine receptors. Université Paris Cité.

Milazzo, M. L., M. N. Cajimat, G. Duno, F. Duno, A. Utrera and C. F. Fulhorst, 2011. Transmission of guanarito and pirital viruses among wild rodents, venezuela. Emerging infectious diseases, 17(12): 2209.

Mills, J. N. and J. E. Childs, 2001. Rodent-borne hemorrhagic fever viruses. Infectious diseases of wild mammals: 254-270.

Moraz, M.-L. and S. Kunz, 2011. Pathogenesis of arenavirus hemorrhagic fevers. Expert review of anti-infective therapy, 9(1): 49-59.

Naveed, M., U. Ali, M. I. Karobari, N. Ahmed, R. N. Mohamed, S. S. Abullais, M. A. Kader, A. Marya, P. Messina and G. A. Scardina, 2022. A vaccine construction against covid-19-associated mucormycosis contrived with immunoinformatics-based scavenging of potential mucoralean epitopes. Vaccines, 10(5): 664.

Obaidullah, A. J., M. M. Alanazi, N. A. Alsaif, H. Albassam, A. A. Almehizia, A. M. Alqahtani, S. Mahmud, S. A. Sami and T. B. Emran, 2021. Immunoinformatics-guided design of a multi-epitope vaccine based on the structural proteins of severe acute respiratory syndrome coronavirus 2. RSC advances, 11(29): 18103-18121.

Ogra, P. L., H. Faden and R. C. Welliver, 2001. Vaccination strategies for mucosal immune responses. Clinical microbiology reviews, 14(2): 430-445.

Organization, W. H., 2004. Laboratory biosafety manual. World Health Organization.

Organization, W. H., 2016. Clinical management of patients with viral haemorrhagic fever: A pocket guide for front-line health workers. Interim emergency guidance for country adaption. World Health Organization.

Peng, C.-X., F. Liang, Y.-H. Xia, K.-L. Zhao, M.-H. Hou and G.-J. Zhang, 2023. Recent advances and challenges in protein structure prediction. Journal of chemical information and modeling, 64(1): 76-95.

Pérez, A., F. J. Luque and M. Orozco, 2012. Frontiers in molecular dynamics simulations of DNA. Accounts of chemical research, 45(2): 196-205.

Pineda, J., D. Brang, E. Hecht, L. Edwards, S. Carey, M. Bacon, C. Futagaki, D. Suk, J. Tom and C. Birnbaum, 2008. Positive behavioral and electrophysiological changes following neurofeedback training in children with autism. Research in autism spectrum disorders, 2(3): 557-581.

Ponomarenko, J., H.-H. Bui, W. Li, N. Fusseder, P. E. Bourne, A. Sette and B. Peters, 2008. Ellipro: A new structure-based tool for the prediction of antibody epitopes. BMC bioinformatics, 9: 1-8.

Pradeepkiran, J. A., S. Sainath, P. K. Balne and M. Bhaskar, 2021. Computational modeling and evaluation of best potential drug targets through comparative modeling. In: Brucella melitensis. Elsevier: pp: 39-78.

Qi, R., H. Yu and X.-J. Yu, 2024. Hemorrhagic fever viruses. In: Molecular medical microbiology. Elsevier: pp: 2479-2493.

Racsa, L. D., C. S. Kraft, G. G. Olinger and L. E. Hensley, 2016. Viral hemorrhagic fever diagnostics. Clinical infectious diseases, 62(2): 214-219.

Radoshitzky, S. R., J. H. Kuhn, P. B. Jahrling and S. Bavari, 2018. Hemorrhagic fever-causing mammarenaviruses. Medical Aspects of Biological Warfare Fort Sam Houston, USA: Borden Institute, US Army Medical Department Center and School, Health Readiness Center of Excellence: 517-545.

Rafi, M. O., K. Al-Khafaji, S. M. Mandal, N. S. Meghla, P. K. Biswas and M. S. Rahman, 2023. A subunit vaccine against pneumonia: Targeting s treptococcus pneumoniae and klebsiella pneumoniae. Network Modeling Analysis in Health Informatics and Bioinformatics, 12(1): 21.

Rahman, M. S., M. K. Rahman, S. Saha, M. Kaykobad and M. S. Rahman, 2019. Antigenic: An improved prediction model of protective antigens. Artificial intelligence in medicine, 94: 28-41.

Rahmani, A., M. Baee, M. Rostamtabar, A. Karkhah, S. Alizadeh, M. Tourani and H. R. Nouri, 2019. Development of a conserved chimeric vaccine based on helper t-cell and ctl epitopes for induction of strong immune response against schistosoma mansoni using immunoinformatics approaches. International Journal of Biological Macromolecules, 141: 125-136.

Ranaghan, M. J., J. J. Li, D. M. Laprise and C. W. Garvie, 2021. Assessing optimal: Inequalities in codon optimization algorithms. BMC biology, 19: 1-13.

Ravikumar, A., C. Ramakrishnan and N. Srinivasan, 2019. Stereochemical assessment of (φ, ψ) outliers in protein structures using bond geometry-specific ramachandran steric-maps. Structure, 27(12): 1875-1884. e1872.

Rosenberg, A. S. and Z. E. Sauna, 2018. Immunogenicity assessment during the development of protein therapeutics. Journal of pharmacy and pharmacology, 70(5): 584-594.

Saha, S., S. Vashishtha, B. Kundu and M. Ghosh, 2022. In-silico design of an immunoinformatics based multi-epitope vaccine against leishmania donovani. BMC bioinformatics, 23(1): 319.

Shafaghi, M., Z. Bahadori, H. Madanchi, M. M. Ranjbar, A. A. Shabani and S. F. Mousavi, 2023. Immunoinformatics-aided design of a new multi-epitope vaccine adjuvanted with domain 4 of pneumolysin against streptococcus pneumoniae strains. BMC bioinformatics, 24(1): 67.

Shamsi, M. H. and H.-B. Kraatz, 2013. Interactions of metal ions with DNA and some applications. Journal of inorganic and organometallic polymers and materials, 23: 4-23.

Shoemaker, T., 2019. Surveillance and epidemiology of viral hemorrhagic fevers (vhfs): Identification of emergence, seroprevelance, and risk factors of vhfs in uganda. Université Montpellier.

Shukla, M., P. Chandley and S. Rohatgi, 2021. The role of b-cells and antibodies against candida vaccine antigens in invasive candidiasis. Vaccines, 9(10): 1159.

Silva-Ramos, C. R., C. Montoya-Ruiz, A. A. Faccini-Martinez and J. D. Rodas, 2022. An updated review and current challenges of *Guanarito virus* infection, venezuelan hemorrhagic fever. Arch virology, 167(9): 1727-1738.

Silva-Ramos, C. R., C. Montoya-Ruíz, Á. A. Faccini-Martínez and J. D. Rodas, 2022. An updated review and current challenges of *Guanarito virus* infection, venezuelan hemorrhagic fever. Archives of virology, 167(9): 1727-1738.

Singh, K., T. T. Khandagale, A. Puri and S. Sinha, 2021. In silico prediction of b-cell and t-cell epitope of ves g 5 and vesp m 5 allergens. Indian journal of allergy, asthma and immunology, 35(2): 72-81.

Singh, S., A. Rao, K. Kumar, A. Mishra and V. K. Prajapati, 2023. Translational vaccinomics and structural filtration algorithm to device multiepitope vaccine for catastrophic monkeypox virus. Computers in biology and medicine, 153: 106497.

Swain, A., 1996. Environmental migration and conflict dynamics: Focus on developing regions. Third world quarterly, 17(5): 959-974.

Tarrahimofrad, H., S. Rahimnahal, J. Zamani, E. Jahangirian and S. Aminzadeh, 2021. Designing a multi-epitope vaccine to provoke the robust immune response against influenza a h7n9. Scientific reports, 11(1): 24485.

Umar, A., A. Haque, Y. Alghamdi, M. Mashraqi, A. Rehman, F. Shahid, M. Khurshid and U. Ashfaq, 2021. Development of a candidate multi-epitope subunit vaccine against klebsiella aerogenes: Subtractive proteomics and immuno-informatics approach. Vaccines. 2021; 9 (11): 1373–92. s Note: MDPI stays neutral with regard to jurisdictional claims in published.

Vishwakarma, P., A. M. Vattekatte, N. Shinada, J. Diharce, C. Martins, F. Cadet, F. Gardebien, C. Etchebest, A. A. Nadaradjane and A. G. de Brevern, 2022. Vhh structural modelling approaches: A critical review. International journal of molecular sciences, 23(7): 3721.

Wahl-Jensen, V., S. R. Radoshitzky, F. de Kok-Mercado, S. L. Taylor, S. Bavari, P. B. Jahrling and J. H. Kuhn, 2013. Role of rodents and bats in human viral hemorrhagic fevers. Viral hemorrhagic fevers: 99-127.

Zaib, S., F. Akram, S. T. Liaqat, M. Z. Altaf, I. Khan, A. A. Dera, J. Uddin, A. Khan and A. Al-Harrasi, 2022. Bioinformatics approach for the construction of multiple epitope vaccine against omicron variant of sars-cov-2. Scientific reports, 12(1): 19087.

Zarychanski, R. and D. S. Houston, 2017. Assessing thrombocytopenia in the intensive care unit: The past, present, and future. Hematology 2014, the American Society of Hematology Education Program Book, 2017(1): 660-666.